International Journal of Rotating Machinery, 9(2): 145–152, 2003

1023-621X/03 $12.00 + .00
DOI: 10.1080/10236210390147461

Taylor & Francis
Taylor & Francis Group

Effects of Volute Design and Number of Impeller Blades on Lateral Impeller Forces and Hydraulic Performance

Daniel O. Baun
Concepts NREC, USA

Ronald D. Flack
Department of Mechanical and Aerospace Engineering, University of Virginia, Charlottesville, Virginia, USA

A comparison is made between the characteristics of the measured lateral impeller forces and the hydraulic performances of a four- and a five-vane impeller, each operating in a spiral volute, a concentric volute, and a double volute. The pump's rotor was supported in magnetic bearings. In addition to supporting and controlling the rotor motion, the magnetic bearings also served as active load cells and were used to measure the impeller forces acting on the pump's rotor. The lateral impeller force characteristics, as a function of a normalized flow coefficient, were virtually identical in the four- and five-vane impellers in each respective volute type. The measured impeller forces for each volute type were compared with correlations in the literature. The measured forces from the double volute configurations agreed with the forces from a correlation model over the full flow range. Single volute configurations compared well with the predictions of a published correlation at high flow rates, $\phi/\phi_n > 0.5$. Concentric volute configurations compared well with a published correlation at low flow rates, $\phi/\phi_n < 0.4$. The head-versus-flow characteristics of the four-vane impeller in each volute type were stable over a greater flow range than the corresponding characteristics of the five-vane impeller. At higher flow rates in the stable region of the head's characteristic curves near the best efficiency point, the five-vane impeller produced higher head than did the four-vane impeller in each volute type.

Keywords centrifugal pump, hydraulic efficiency, impeller forces, magnetic bearings

Pumps are used in varied applications and are integral to many industries. Yet, in spite of their prevalence and relatively simple configurations compared to other turbomachines, designing an efficient and durable pump remains a challenge. Two effects that challenge a designer are the force loads on the impeller and the hydraulic efficiency. Small changes in the volute design have been shown to affect one or both of these parameters significantly (Baun 2000). If force loads are too high, premature failure of bearings or other components can take place. If the efficiency is too low, the energy consumption over the life of the pump can cost an industry a significant amount of money (Hergt 1999). This article deals with both issues.

One of the earliest archived investigations of static, or time-averaged, hydraulic lateral forces acting on centrifugal pump impellers was by Binder and colleagues (1936). Stepanoff (1957) presents a simple force model based on impeller geometry, pump operating head, and the normalized pump capacity for the calculation of resultant radial forces. Agostinelli and colleagues (1960) modified Stepanoff's model to account for the effect of specific speed on radial forces. Hergt and Krieger (1972) made impeller static force measurements in a vaned diffuser pump. They also investigated the effect of small impeller eccentricities on the forces. Guelich and colleagues (1987) presented an overview of static and dynamic forces in centrifugal pumps. A brief discussion of the static forces in various types of pumps—single volute, double volute, concentric, and diffuser—is given. The force correlations of the Hydraulics Institute have been used

Received 28 March 2002; accepted 28 March 2002.
This research was sponsored by the Rotating Machinery and Controls (ROMAC) Industrial Research Program at the University of Virginia, Charlottesville, Virginia, USA.
Address correspondence to Daniel O. Baun, Concepts NREC, E-mail: dob@conceptsnrec.com

for decades and were most recently updated in 1994. Despite the relatively long history of literature documenting impeller forces in pumps, there are few detailed investigations into the effects of various impeller and volute combinations on these forces with a parallel examination of the hydraulic performance.

Over the past few years, great strides have been made in Computational Fluid Dynamics (CFD). However, the analysis as applied to a pump has not yet developed to a level permitting design solely on the basis of computational results. Experimental data for the internal flow are needed to verify computational results. Benchmark velocity data over a wide range of geometries are needed to understand the flow mechanics and to verify CFD predictions.

This article presents a set of directly measured (using active magnetic bearings as load cells) impeller lateral force data for three different volute configurations: a spiral volute, a concentric volute, and a double volute. The force data are presented with two different impeller configurations—a four-vane impeller and a five-vane impeller. In addition, the hydraulic performance of the two impeller designs are compared in each of the three different volute configurations. The performance and force data complement the fundamental velocity and pressure data of de Ojeda and colleagues (1995) and Miner and colleagues (1989) for some of the same geometries. The data herein, complemented by the previous fundamental data, represent the most complete data available in the literature for conventional centrifugal pumps.

TEST APPARATUS

The pump apparatus and flow loop used in this research were described in detail by Baun and Flack (1999). The pump rotor, Figure 1, is supported radially and axially by magnetic bearings that also serve as active load cells for the measurement of hydraulic forces. The static and dynamic properties of the load cells (magnetic bearings) were characterized and documented by Fittro and colleagues (1997).

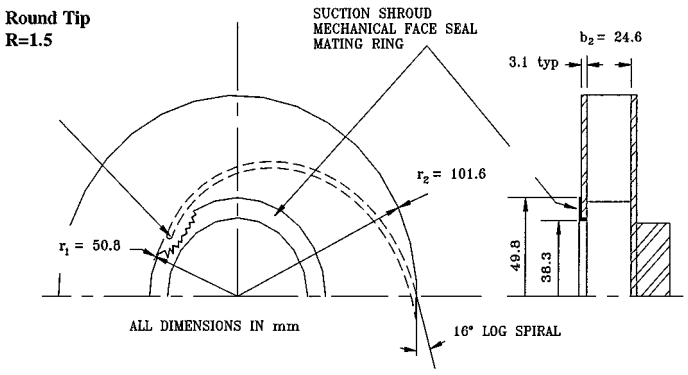

FIGURE 2
Impeller.

A typical static/time–averaged impeller force measurement proceeded as follows. First, a set of static bearing references, or tare forces, were obtained by operating the pump with a blank disk installed in place of the impeller. The blank had the same inertial properties, an identical stuffing box, and identical suction shroud seals as the actual impeller. The reference forces were then subtracted from the bearing reaction forces obtained with the impeller. This technique of subtracting an appropriate tare force measurement from each impeller force measurement removed any biasing effects due to seal or coupling reactions as well as the rotor weight.

The details of the pump hydraulic design are given in Figures 2, 3, 4, and 5: the impeller, the spiral volute casing, the concentric volute casing, and the double volute casing, respectively. The impeller shown in Figure 2 was constructed with both four and five vanes. The pump casing consisted of a radially split pressure chamber into which the volute inserts (Figs. 4, 5,

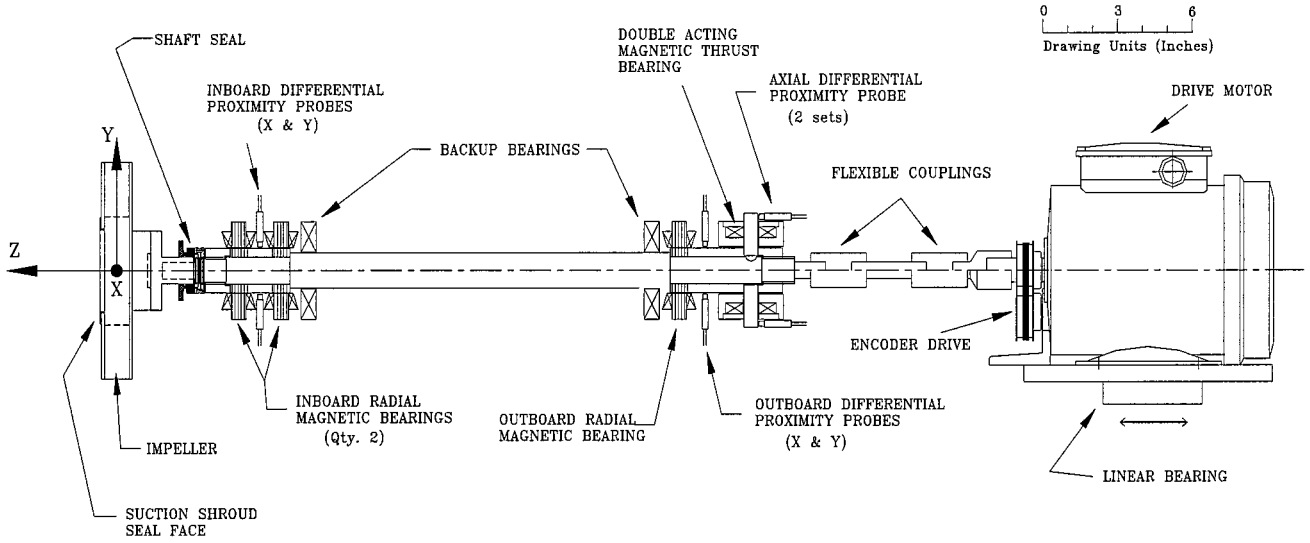

FIGURE 1
Test rotor.

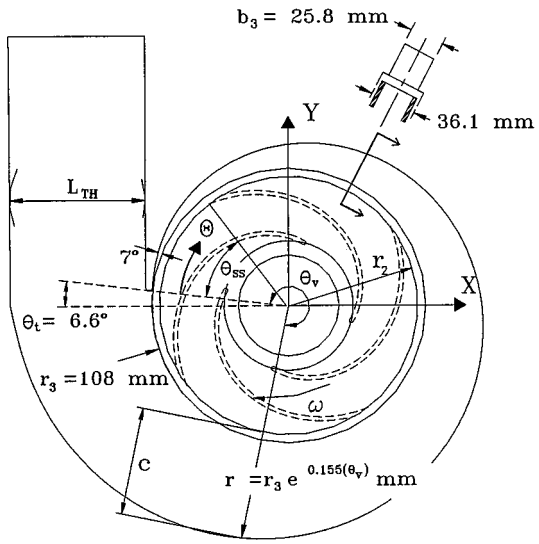

FIGURE 3
Spiral volute.

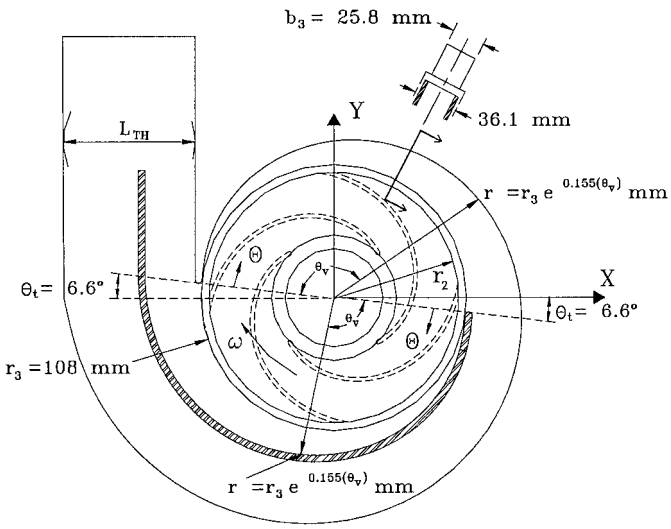

FIGURE 5
Double volute.

and 6) were installed. The flow-path profiles for the various volute inserts were cut from Plexiglas sheets using a numerically controlled milling machine and have a two-dimensional cross-section, as shown in Figures 3, 4, and 5. The volute throat areas, $A_{th} = L_{th} \times b_3 = 2785$ mm^2 (4.3 in^2), are identical between the concentric and the spiral volute casings. The double volute casing was realized by inserting a splitter in the spiral volute to produce two symmetrical spiral flow paths 180 degrees apart.

The pump's volumetric flow rate was measured using a sharp-edged orifice. The normalized flow measurement uncertainty, $\Delta\phi/\phi_n$, varied from approximately $\pm$ 0.045 at low flow near shut-off to approximately $\pm$ 0.005 at high flow near the best efficiency point (BEP). The static differential pressure developed across the pump was measured and corrected for velocity head based on the measured flow rate to obtain the total discharge head. The normalized head measurements uncertainty, $\Delta\Psi/\Psi_n$, was approximately $\pm$ 0.005. To determine the efficiency characteristics of the various impeller-volute combinations, the input or shaft power, P, was required. The motor's electric power was first calibrated against a dynamometer test of the motor's output or shaft power. During subsequent pump performance tests the measured electrical power was used to calculate the motor's output power based on the motor's calibration function. The normalized uncertainty, $\Delta\eta/\eta_n$, for the efficiency measurements was approximately $\pm$ 0.01 at low flows near shut-off and approximately $\pm$ 0.005 at high flows near the BEP.

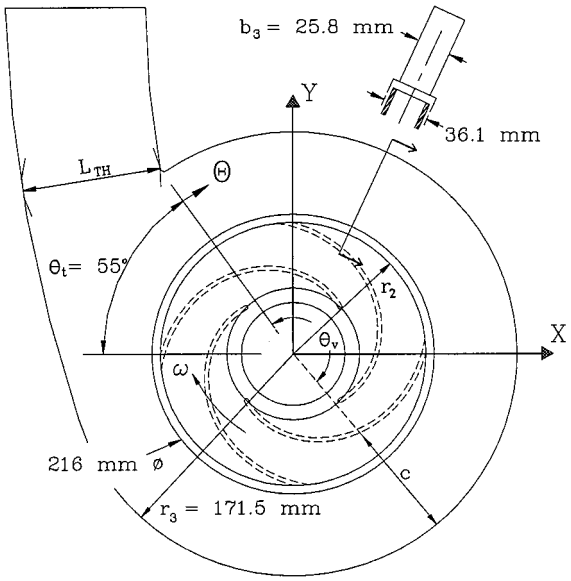

FIGURE 4
Concentric volute.

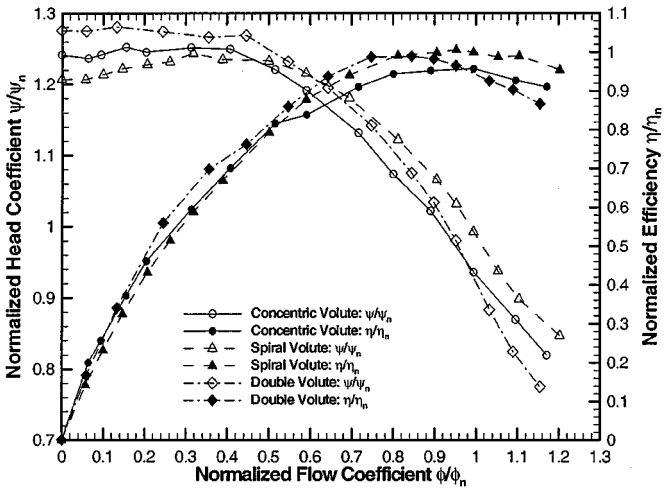

FIGURE 6
Four-vane impeller; hydraulic performance.

RESULTS

Hydraulic Performance

The hydraulic performance of the four-vane impeller in the spiral volute served as the baseline case for comparison with all other impeller-volute combinations. The four-vane impeller–spiral volute combination was selected as the baseline configuration for historical reasons: Miner and colleagues (1989) and de Ojeda and colleagues (1995). The best efficiency head and flow coefficients for the four-vane impeller–spiral volute combination, $\Psi_{4SV,BEP} \equiv \Psi_n$ and $\phi_{4SV,BEP} \equiv \phi_n$, respectively, are used to normalize all head and flow coefficient data. To facilitate simple and direct comparison of the efficiency between all volute-impeller combinations, all efficiencies were normalized by the efficiency of the four-vane impeller–spiral volute combination at the design flow, which corresponds to the BEP and hence is symbolized by $\eta_{4SV,BEP} \equiv \eta_n$. The mechanical set-up, stuffing box seal, suction shroud seal, magnetic bearings, couplings and shroud clearances were the same for all volute-impeller combinations. Therefore, normalized efficiencies greater than one, $\eta/\eta_n > 1$, represent an increase in hydraulic efficiency, whereas normalized efficiencies less than one, $\eta/\eta_n < 1$, represent a decrease in hydraulic efficiency relative to the baseline. The nominal design point of the four-vane impeller in the spiral volute is 6.3 liters/sec (100 USgpm) at 2.03 m (6.66 ft) total dynamic head at an operating speed of 620 rpm. These parameters give a design specific speed, $N_s = 0.547$ (1495 US units [rpm USgpm$^{0.5}$/ft$^{0.75}$]), a design flow coefficient, $\phi_n = 0.061$, and a design head coefficient, $\Psi_n = 0.458$.

Figure 6 shows the normalized head coefficient, Ψ/Ψ_n, and normalized efficiency, η/η_n, versus the normalized capacity, ϕ/ϕ_n, for the four-vane impeller operating in each of the three volutes. The concentric volute has a flat head characteristics for $\phi/\phi_n < 0.4$ and therefore an improvement in stability over the baseline spiral volute. The head developed by the concentric volute is consistently lower than that of the spiral volute for $\phi/\phi_n > 0.6$ and, consequently, a reduced efficiency in the same flow range is observed. The peak normalized efficiency, η/η_n, for the concentric volute is approximately 0.95 and occurs at $\phi/\phi_n \approx 0.95$. The double volute has a continuously rising head characteristic and is therefore the most stable characteristic of the three configurations shown in Figure 6. The peak normalized efficiency, η/η_n, for the double volute is approximately 0.99 and occurs at $\phi/\phi_n \approx 0.8$. For $\phi/\phi_n > 0.8$, the efficiency and head characteristics for the double volute drop rapidly as compared to the corresponding characteristics of the spiral volute and the concentric volute. The reason for the shift in the best efficiency point to a lower flow rate and for the relatively rapid droop in the head and efficiency characteristics of the double volute at high flows is likely to be the result of increased volute losses. The losses in the double volute will increase over the single volute because of more wetted surface and two tongues, which result in twice the incidence losses as compared to the single volute. In addition, the splitter (which forms the double volute from the single volute) will add blockage in the volute, thus increasing the flow velocities at any given flow rate. This has the combined effect of increasing skin friction losses and also shifting the matching point of the impeller-volute combination to a lower flow rate.

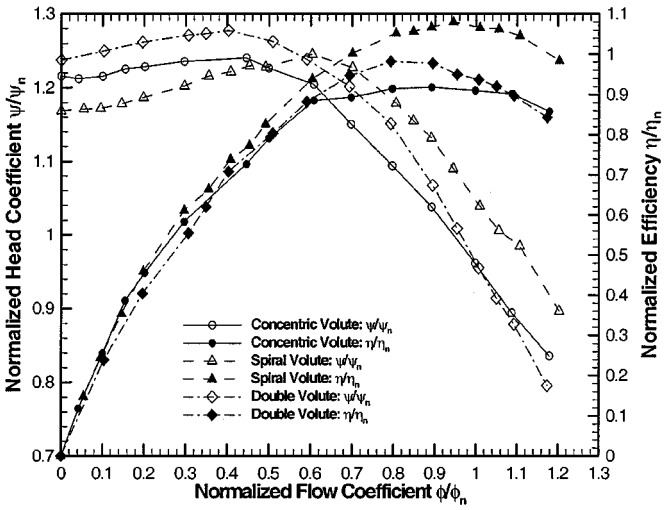

FIGURE 7
Five vane impeller; hydraulic performance.

Figure 7 shows the normalized head coefficient and normalized efficiency versus the normalized capacity, for the five-vane impeller operating in each of the three volute configurations. The performance characteristics of the four-vane impeller operating in each volute type, as illustrated in Figures 6 and discussed above, will be used as a references for comparison with the five-vane impeller in each respective volute. Compared to the four-vane impeller, the shut-off head coefficient for the five-vane impeller operating in each volute decreased. The unstable zone for the spiral volute increased to include the region $\phi/\phi_n < 0.6$, while the head characteristic for the concentric volute went from being neutrally stable or flat to unstable for $\phi/\phi_n < 0.4$. The head characteristic for the double volute has become unstable for $\phi/\phi_n < 0.4$. For normalized flow rates above approximately 0.6, the five-vane impeller developed higher head than the four-vane impeller in each volute configuration. Table 1 lists

TABLE 1
Head and Efficiency Comparison at BEP

	Four-vane impeller		Five-vane impeller	
	Ψ/Ψ_n	η/η_n	Ψ/Ψ_n	η/η_n
Spiral volute $\phi/\phi_n = 1.0$	1.0	1.0	1.05	1.07
Concentric volute $\phi/\phi_n = 0.95$	0.97	0.95	1.0	0.92
Double volute $\phi/\phi_n = 0.8$	1.115	0.99	1.145	0.98

the normalized head coefficient and normalized efficiency for each impeller type in each volute at the normalized flow coefficient corresponding to the BEP of each configuration. While it is not possible to definitively explain the reasons for the observed increase in the head characteristic at the BEP with the five-vane impeller, without a detailed investigation of the internal flow field, a likely explanation is a reduction in the impeller slip with an increase in the number of impeller blades (Pfleiderer 1961). The observed changes in the efficiency characteristic at the BEP between the four- and five-vaned impellers cannot be accounted for with the current level of investigation.

RESULTS

Radial Forces

Figure 8 shows the lateral force data for the four-vane impeller–spiral volute combination resolved into the X and Y coordinate directions. The coordinate directions are shown in Figure 3. In addition, uncertainty bars on each data point are given. The uncertainty bars represent ± 95% confidence intervals and are the total or cumulative uncertainties in each parameter. The cumulative uncertainty is the sum of the uncertainties due to transducer calibration and the random uncertainty due to averaging multiple transducer readings at each set point. The uncertainty in the subsequent force magnitude data, ΔF, and the force vector orientation data, $\Delta\theta_f$, can be reasonably approximated as $\Delta F \approx \Delta F_x \approx \Delta F_y$ and $\Delta\theta_f \approx \Delta F/F$, respectively.

Figures 9 and 10 show the nondimensional force magnitude, F, and force vector orientation, θ_f, versus the normalized flow coefficient, ϕ/ϕ_n, for the four-vane impeller and the five-vane impeller in each volute configuration. The force vector orientation, θ_f, is referenced from the volute tongue in the Θ coordinate direction, positive in the direction of impeller rotation. The force magnitude characteristic for the four-vane impeller in the spiral volute, Figure 9, is nearly identical to that of the five-vane impeller, Figure 10. Figure 11 is a direct comparison between the four- and five-vane impellers in the spiral volute. The five-vane impeller force characteristic has a slightly higher magnitude for $\phi/\phi_n < 1.05$ and is more rounded in the $0.95 < \phi/\phi_n < 1.05$ flow range. The force correlation given by the Hydraulic Institute (1994) for a spiral volute is included in Figure 11 for comparison. The force orientation for the four-vane impeller in the spiral volute, Figure 9, is virtually identical to that for the five-vane impeller except in the $0.90 < \phi/\phi_n < 1.10$ flow region. The large swing in the force orientation centered at the design flow occurs over a wider flow range for the five-vane impeller than

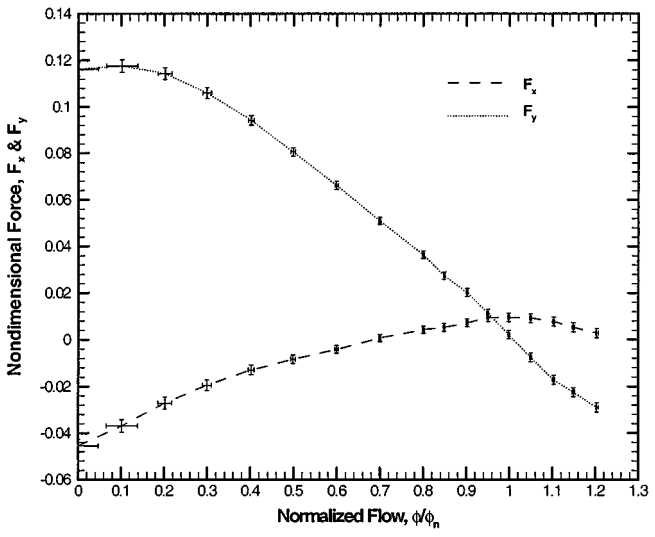

FIGURE 8
Measurement uncertainties: ΔF_x, ΔF_y, $\Delta\varphi/\varphi_n$.

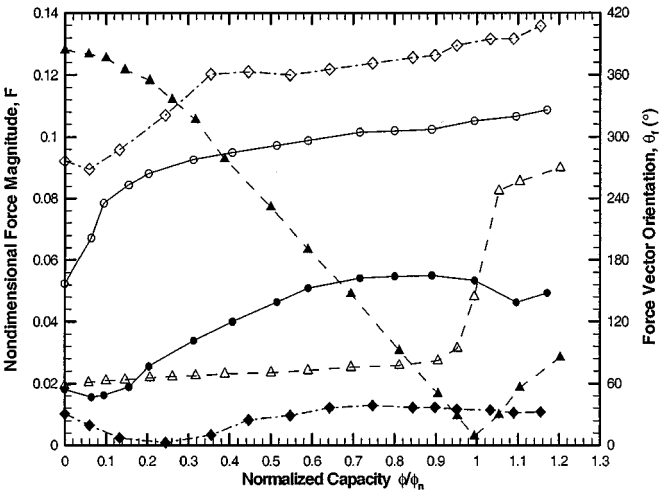

FIGURE 9
Four-vane impeller. Force characteristics (F): △, spiral volute; ○, concentric volute; ♢, double volute. Force orientation (θ_f); ▲, spiral volute; ●, concentric volute; ♦, double volute.

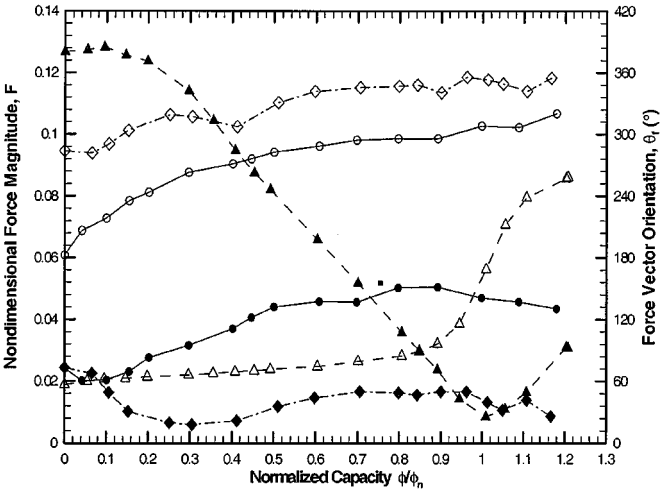

FIGURE 10
Five-vane impeller. Force characteristics (F): △, spiral volute; ○, concentric volute; ♢, double volute. Force orientation (θ_f); ▲, spiral volute; ●, concentric volute; ♦, double volute.

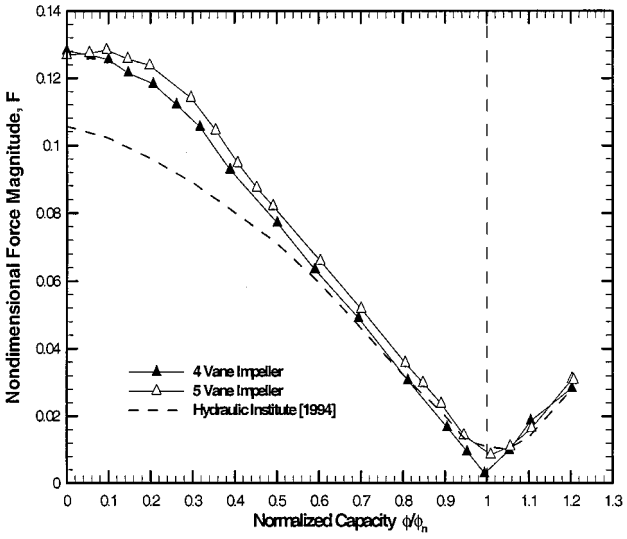

FIGURE 11
Spiral volute; resultant impeller forces.

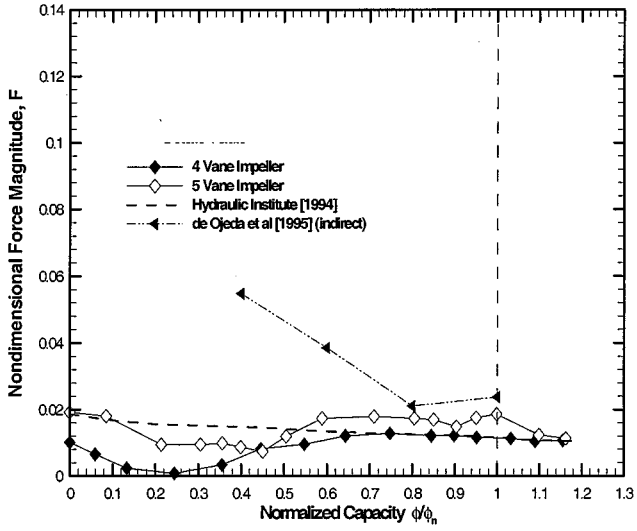

FIGURE 13
Double volute; resultant impeller forces.

for the four-vane impeller and consequently appears to be more gradual.

The force magnitude characteristic for the four-vane impeller in the concentric volute, Figure 9, is identical to that for the five-vane impeller, Figure 10. A direct comparison between the two impellers is given in Figure 12. Also shown in Figure 12 is an early empirical correlation by Biheller (1965) for concentric volutes. For $\phi/\phi_n < 0.4$ Biheller's correlation and the current measurements are virtually identical. However, above this flow range Biheller's empirical correlation overpredicts the force magnitude as compared to the measurements. The force orientation of the four-vane impeller in the concentric volute, Figure 9, is identical to its counterpart for the five-vane impeller, Figure 10, except in the region $\phi/\phi_n < 0.1$. The four-vane impeller has a shutoff force orientation, $\theta_f = 145^\circ$, while the five-vane impeller has a shutoff force orientation, $\theta_f = 180^\circ$. This difference may be an artifact of measurement uncertainty and small force magnitudes.

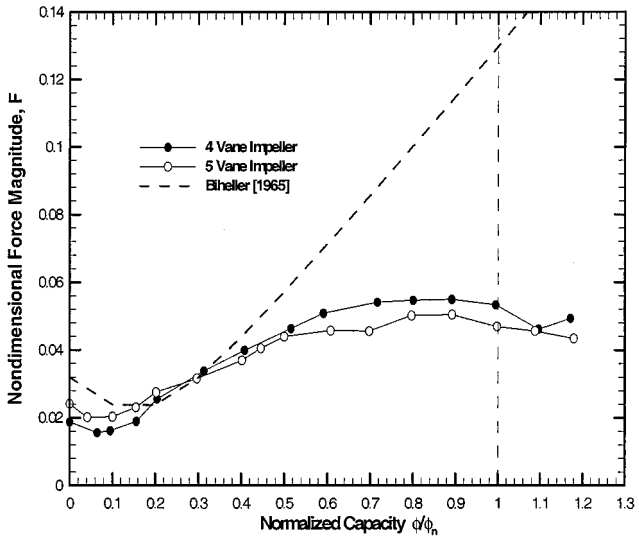

FIGURE 12
Concentric volute; resultant impeller forces.

The force magnitude for the four-vane impeller in the double volute in Figure 9 is similar to the corresponding characteristic for the five-vane impeller, Figure 10. Figure 13 is provided to show as a direct comparison between the force magnitudes of the four- and five-vane impellers in the double volute. The force magnitude of the five-vane impeller is almost constant in value, $F \approx 0.02$, over the whole flow range, which is slightly higher than that of the four-vane impeller. An empirical correlation for the hydraulic force in double volute pumps from the Hydraulic Institute (1994) is also included in Figure 13. Impeller force data as calculated by de Ojeda and colleagues (1995) is also included. The force data were obtained by integrating shroud pressure measurements at discrete angular positions around the impeller periphery. Near the design flow, $\phi/\phi_n = 1.0$, the data from de Ojeda are slightly (0.004) higher than the current five-vane impeller force data, and about 0.01 higher than the four-vane impeller force data. For $\phi/\phi_n < 0.8$, the data from de Ojeda and colleagues (1995) increase in magnitude and are about three times higher than the current data, at $\phi/\phi_n = 0.4$. The large difference between the data from de Ojeda and colleagues (1995) and the current measurements is likely to be due to (1) contributions to the impeller force from asymmetrical momentum flux distributions that are not included in the data from de Ojeda and colleagues (1995); (2) the inherent limitations of accurately predicting the impeller force from the integration of a small number of discrete shroud-pressure measurements. The force vector orientations for the four-vane impeller in the double volute, Figure 9, differ slightly from the corresponding force vector orientations for the five-vane impeller, Figure 10, especially at

higher flow rates. These differences may be the result of higher uncertainties in the force orientation vector due to the lower magnitude of the measured forces ($\Delta\theta_f \approx \Delta F/F$).

SUMMARY

A set of directly measured (using active magnetic bearings as load cells) impeller force data for a 0.547-specific speed pump with three different volute configurations (a spiral volute, a concentric volute, and a double volute) and two different impeller configurations (a four-vane impeller and a five-vane impeller) are presented herein. The hydraulic performances of the two impeller designs are compared in each of the three different volute configurations. Although the exact force magnitude and hydraulic performance are dependent on the exact geometric details of a pump design, the data presented in this paper are representative of the trends for the generic types tested. The force and performance data complement the velocity and pressure data from the University of Virginia for some of the same geometries. When complemented with the previous fundamental data, the data herein represent the most complete data available in the literature for conventional centrifugal pumps. These data can be used as benchmarks for validating numerical predictions.

The lateral impeller force characteristics, as a function of the normalized flow coefficient, were virtually identical for the four- and five-vane impellers in each respective volute type. The measured impeller force characteristics for each volute type were compared with correlations from the literature. The lateral force characteristics for the spiral volute configurations compared well with the force distribution modeled by the Hydraulics Institute for $\phi/\phi_n > 0.5$. For lower flows, $\phi/\phi_n < 0.5$, the measured force characteristic was as much as 17% larger than the force magnitude predicted from the Hydraulics Institute correlation. The force characteristics for the concentric volute configurations were compared to a correlation from Biheller. At low flow coefficients, $\phi/\phi_n < 0.4$, the correlation accurately predicted the radial forces. However, at higher flow rates the correlation by Biheller over predicted the radial force magnitude. At the design flow coefficient, $\phi/\phi_n = 1.0$, the correlation predicted a force magnitude more than two times the measured force. The measured impeller force characteristics for the double-volute configurations compared very well with the force distribution modeled by the correlation from the Hydraulics Institute.

The head-versus-flow characteristic of the four-vane impeller in each volute type was stable (had a negative slope) over a wider flow range than the corresponding characteristic for the five-vane impeller in each volute type. The four-vane impeller in the spiral volute had an unstable characteristic for $\phi/\phi_n < 0.4$, whereas the head characteristic for the five-vane impeller in the spiral volute was unstable for $\phi/\phi_n < 0.6$. The four-vane impeller in the double volute combination was stable right up to shut-off. However, the characteristic for the five-vane impeller in the same volute was unstable for $\phi/\phi_n < 0.4$. At higher flow rates in the stable region (negative slope) of the head characteristic curves, the five-vane impeller produced higher head than did the four-vane impeller in each volute type. This was especially true for five-vane impeller–spiral volute combination, where a 5% increase in head was observed, as compared to the four-vane impeller–spiral volute combination.

NOMENCLATURE

BEP	best efficiency point
b_2	flow passage width at impeller exit
c_{m2}	radial velocity at impeller exit ($Q/(2\pi r_2 b_2)$)
F	nondimensional force ($F_{\text{dim}}/(\rho\pi r_2^3\Omega^2 b_2)$
g	acceleration of gravity
H	pump total discharge head
N_s	specific speed ($\Omega Q^{0.5}/(Hg)^{0.75}$)
P	input power
Q	pump volume flow rate
r_2	impeller outer radius
u_2	impeller peripheral velocity (Ωr_2)
X, Y, Θ	coordinate directions
Δ	uncertainty (generic)
ϕ	flow coefficient (c_{m2}/u_2)
Ψ	head coefficient (Hg/u_2^2)
Ω	impeller angular velocity
θ_f	force vector orientation
ρ	fluid density
η	hydraulic efficiency ($\rho g H Q/P$)

Subscript

n	reference condition: BEP of four-vane impeller, spiral volute combination

REFERENCES

Agostinelli, A., Nobles, D., and Mockridge, C. R. An experimental investigation of radial thrust in centrifugal pumps. *ASME Journal of Engineering for Power*. April 1960, pp. 120–126.

Baun, D. O., and Flack, R. D. 1999. A plexiglas research pump with calibrated magnetic bearing/load cells for radial and axial hydraulic force measurements. *ASME Journal of Fluids Engineering* 121:126–132.

Baun, D. O., Kostner, L., and Flack, R. D. 2000. Effect of relative impeller-to-volute position on hydraulic efficiency and static radial force distribution in a circular volute centrifugal pump. *ASME Journal of Fluids Engineering* 122:598–603.

Biheller, H. J. 1965. Radial forces on the impeller of centrifugal pumps with volute, semivolute, and fully concentric casings. *ASME Journal of Engineering for Power*. July 1965, pp. 319–323.

Binder, R. C., and Knapp, R. T. 1936. Experimental determination of the flow characteristics in the volutes of centrifugal pumps, 649–661. *Transactions of the ASME*, Vol. 58, Nov 1936, pp. 648–661.

de Ojeda, W., Flack, R. D., and Miner, S. M. 1995. Laser velocimetry measurements in a double volute centrifugal pump. *International Journal of Rotating Machinery* 1:199–214.

Fittro, R. L., Baun, D. O., Maslen, E. H., and Allaire, P. E. 1997, June. Calibration of an 8-pole planar radial magnetic actuator. *Paper 97-GT-108, ASME Gas Turbine Conference*. Orlando, FL.

Guelich, J., Jud, W., and Hughes, S. F. 1987. Review of parameters influencing hydraulic forces on centrifugal impellers. *Proceedings of the Institution of Mechanical Engineers* 201:163–173.

Hergt, P. 1999. Pump research and development: past, present, and future. *ASME Transactions, Journal of Fluids Engineering* 121:248–253.

Hergt, P., and Krieger, P. 1972. Radial forces in centrifugal pumps with guide vanes. *Proceedings of the Institution of Mechanical Engineers* 184:101–107.

Hydraulic Institute. 1994. American national standard for centrifugal pumps for nomenclature, definitions, application and operation. ANSI/HI. Vol. 1.1–1.5, pp. 103–104, Calculation of Radical Thrust for Centrifugal Pumps.

Miner, S. M., Beaudoin, R. J., and Flack, R. D. 1989. Laser velocimeter measurements in a centrifugal flow pump. *ASME Transactions, Journal of Turbomachinery* 111:205–212.

Pfleiderer, C. 1961. *Die Kreiselpumpen*. Berlin: Springer-Verlag.

Stepanoff, A. J. 1957. *Centrifugal and Axial Flow Pumps*, New York: Wiley.